# Variable-Volume Hollow-Fiber Enzyme Reactor with Pulsatile Flow

Hollow-fiber device has been used to investigate the effect of ultrafiltration swing on the performance of membrane-enzyme reactor. Experiments with $\beta$-galactosidase and ONPG have shown that bidirectional ultrafiltration induced by pulsatile flow gives rise to an increase in conversion relative to that obtained at steady operation without ultrafiltration swing. This increase apparently comes from the enhanced mass transfer due to ultrafiltration.

**IN HO KIM and HO NAM CHANG**

Department of Chemical Engineering
Korea Advanced Institute of Science and Technology
Seoul, Korea

## SCOPE

Recently it has been theoretically shown that the ultrafiltration swing in membrane-enzyme reactor may improve the performance of the reactor as compared to the steady operation (Kim and Chang, 1983). In the present work a hollow fiber module was selected to carry out a continuous ultrafiltration swing operation experimentally without explaining the results with the CSTR model proposed by the authors. The bidirectional ultrafiltration can be induced by inducing a pulsatile flow at the inlet and keeping the outflow constant at the time-averaged inflow rate. The amplitude and the period were varied to change the convectional transport rate relative to the diffusional transport rate through membrane. In addition, feed concentration and enzyme loading in the shell side of the hollow fiber module were adopted as variables for investigating their influence on the degree of diffusion limitation.

## CONCLUSIONS AND SIGNIFICANCE

The experimental results show that one can indeed obtain a substantial increase in conversion by introducing ultrafiltration to the conventional hollow-fiber enzyme reactor. From the permeability data calculated from steady conversions, the ratio of convective to diffusive fluxes can be determined. Conversion increased with the increase of the flow amplitude, while it little depended on the period. The increase of conversion relative to that of the steady operation was limited because there existed a maximum allowable pressure for fibers, and some part of the enzyme solution in the shell was entrapped more favorably in the sponge region of the fiber. The latter limitation reduces the apparent transport resistances of substrate in the shell side, which in turn increases the conversion of the steady operation at a given membrane permeability with zero enzyme loading.

### INTRODUCTION

During the past ten years hollow fiber membrane devices have been examined as a possible candidate for an immobilized enzyme reactor. Rony (1971) was perhaps the first to suggest the hollow fiber device for retaining enzyme in the lumen of fiber. Rony (1972) also reported experimental data obtained in a hollow fiber beaker using alkaline phosphatase and chymotrypsin.

On the other hand, Waterland et al. (1974, 1975) placed an enzyme in the sponge region of hollow fibers and let a substrate flow through the lumen. Silman et al. (1980) recirculated multienzyme solution in the shell side by a pump to mix a crude extract of $\alpha$-galactosidase and invertase. In all the above investigations diffusion was apparently the dominant mechanism for substrate transport (Lewis and Middleman, 1974).

Ku et al. (1981) supplied air to mammalian cell culture system in a hollow fiber device by the pulsed pressure method. Recently, Kim (1982) devised the flow swing operation in membrane-enzyme reactor after performing a series of investigations on the roles of ultrafiltration in membrane devices. Also Kim and Chang (1983) have theoretically shown that ultrafiltration swing induced by the pulsed flow method as well as the pressure swing increases the conversion and virtually removes diffusion limitation in a continuous CSTR-type membrane-enzyme reactor system. The effectiveness of this operation depends on the relative increase of the convectional transport due to ultrafiltration over the diffusion-moderated transport. In the present experimental study we shall examine the effect of the flow-induced ultrafiltration in a hollow fiber module on the conversion and show that this new type of reactor operation gives more conversion than the conventional diffusion-moderated hollow fiber reactor using $\beta$-galactosidase and ONPG.

### MATERIALS AND METHODS

#### Hollow Fiber Module

Amicon hollow fiber system (Model $CH_4$) and fiber bundles (H1P5 and H1P10) were used throughout the experiment. Fiber characteristics are as follows:

Correspondence concerning this paper should be addressed to Ho Nam Chang.

| | H1P5 | H1P10 |
|---|---|---|
| Inside Diameter | 0.05 cm | 0.02 cm |
| Outside Diameter | 0.1 cm | 0.035 cm |
| Surface Area | 560 $cm^2$ | 930 $cm^2$ |
| Fiber Number | 250 | 1,000 |
| Nominal Mol Wt. Cutoff | 5,000 | 10,000 |

#### Enzyme

Crystalline suspension form of $\beta$-galactosidase obtained from *E. coli* was purchased from Sigma Chemical Co. This enzyme is sufficiently large enough (M.W. 540,000) not to leak through the fiber walls. The activity was measured at 25°C in accordance with the recommendation of the supplier.

#### Substrate

O-Nitrophenyl-$\beta$-D-galactopyranoside (ONPG, Sigma Chemical Co.) was dissolved in 0.1 M phosphate buffer (pH 7.25 ± 0.01).

#### Experimental Setup

Schematic experimental apparatus is shown in Figure 1. Substrate solution was delivered to the tube side in two modes. When the reactor was operated without the ultrafiltration swing, one of the inlet pumps was run to feed the substrate into the reactor. Three-way valve was rotated so that the reactor effluent passed directly through a flow cell in spectrophotometer (Beckman, Model 35). For the cyclic operation, the three-way valve was connected to the outlet pump, and the outlet flow rate was set to the mean value of pulsatile inlet flow rate. A time switched one pump and the other periodically and produced a pulsed inflow of square wave. Volume change in the shell side was monitored by a graduated cylinder where also a part of enzyme solution was retained. Concentration histories of the product were recorded on chart papers.

#### Operating Procedure

Used enzyme solution in the shell side was denatured by recirculating 6 M urea solution. After draining the denatured enzyme solution, phosphate buffer solution was ultrafiltered from the tube side to the shell side of hollow fiber module. In accordance with the method of Kohlwey and Cheryan (1981), bovine serum albumin was used to pretreat the fiber, followed by filling the shell and the graduated cylinder with the enzyme solution. The substrate solution was prepared in 0.1 M phosphate buffer, 0.1 M mercaptoethanol, and 1 mM $MgCl_2$. The solution temperature was set to 25°C in a constant water bath before entering into the fiber bundle. Conversion was calculated by dividing the absorbance of the product, o-nitrophenol (ONP) at 405 nm, by 2.7 which is the millimolar extinction coefficient at pH 7.25. Since ONP is strongly absorbed on the fiber, the steady conversion was taken after no further change in the conversion was observed.

#### Kinetic Parameter Determination

Initial reaction rate was tasken in a thermostated sipper cell of Bauch and Lomb spectrophotometer (Model 88), and the kinetic constant $K_m$ and $K_I$ were determined from a double reciprocal plot of initial reaction rate vs. substrate concentration by varying the galactose concentration. As a complementary experiment, the absorbance reading with time was recorded and put into the integral form of Michaelis-Menten equation to confirm the parameter obtained from the initial reaction rate method.

#### Determination of Hollow Fiber Permeability

Permeability measurements were made by recirculating a solution containing ONPG through the interior of fibers. Distilled water was used as dialysate and recirculated countercurrently outside the fibers. Care was taken to eliminate the mass transfer due to ultrafiltration. Concentration of ONPG was assayed using a total organic carbon analyzer (Beckman, Model 915-B). Permeability can be calculated through the following equation (Colton et al., 1971).

$$\ln \frac{C_{Bi} - C_{Di}}{C_b - C_d} = \frac{2K_oAt}{V} \tag{1}$$

where $K_o$ represents overall membrane permeability. The overall membrane resistance consists of three terms, i.e., that of membrane ($1/k_m$), the tube-side liquid film ($1/k_{Lt}$) and the shell-side liquid film ($1/k_{Ls}$). Accordingly,

$$1/K_o = 1/k_{Lt} + 1/k_m + 1/k_{Ls} \tag{2}$$

As discussed by Kataoka et al. (1980), $k_{Lt}$ can be calculated by the Lêvêque's solution given by

$$(k_{Lt}/u)(Sc^{2/3}) = 1.61Re^{-2/3}(L/d)^{-1/3} \tag{3}$$

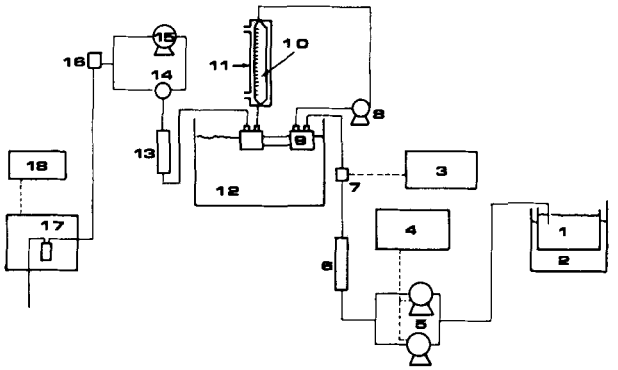


**Figure 1. Experimental apparatus.**

1. Feed tank 2. Water bath 3. Recorder 4. Timer
5. Inlet peristaltic pump 6. Inlet rotameter
7. Pressure transducer 8. Bellow pump
9. Hollow fiber module 10. Graduated cylinder
11. Water jacket 12. Water bath
13. Outlet rotameter 14. Three way valve
15. Outlet peristaltic pump 16. Bubble trap
17. Spectrophotometer 18. Recorder

#### Determination of Permeability in Presence of Reaction

When we fill the shell side with the enzyme solution, the enzyme remains in the sponge region of the fibers preferentially rather than in the bulk solution of the shell side so that the substrate concentration profile in the sponge region becomes steeper than that without the enzyme reaction. Hence the overall resistance obtained from the conversion data might be smaller than that from the dialysis experiment. To determine the permeability from the conversion data, the following mass balance equations are set up around the fiber walls

$$-Q\frac{dC_t}{dx} - \frac{K_oA}{L}(C_t - C_s) = 0 \tag{4}$$

$$K_oA\left[\frac{1}{L}\int_0^L C_t dx - C_s\right] - \frac{V_sV_mC_s}{K_m + C_s} = 0 \tag{5}$$

where $C_t$ and $C_s$ represent the concentrations in the tube and the shell, respectively. Equations 4 and 5 are solved with the boundary condition of $C_t = C_o$ at $x = 0$. The resulting solutions are

$$\frac{C_s}{C_o} = \frac{1}{2}\left[-\left(\frac{K_m}{C_o} - \frac{V_sV_m}{QC_o}\Phi\right) + \sqrt{\left(\frac{K_m}{C_o} - \frac{V_sV_m}{QC_o}\Phi\right)^2 + 4\frac{K_m}{C_o}}\right] \tag{6}$$

$$\frac{C_t - C_s}{C_o - C_s} = \exp\left(-\frac{K_oAx}{QL}\right) \tag{7}$$

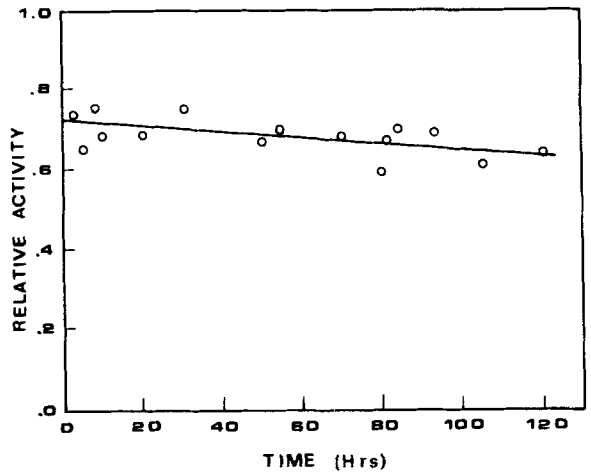


Figure 2. Storage stability of enzyme in shell side of hollow fiber module.

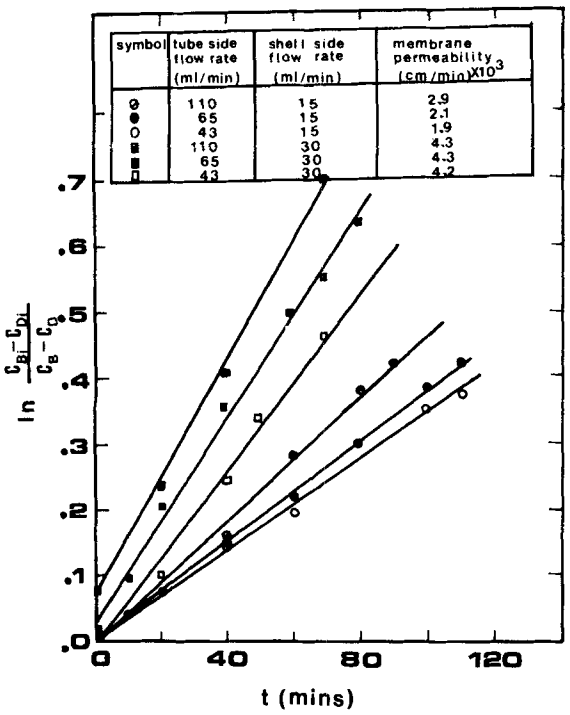


Figure 3. Measurement of permeability for H1P5 fiber by dialysis experiment.

where

$$\Phi = [\exp(-K_o A/Q) - 1]^{-1} \quad (8)$$

Using Eqs. 6 and 7, permeability can be calculated by trial and error method with the conversion data.

## RESULTS AND DISCUSSION

The Michaelis-Menten constant, $K_m$ and the inhibition coefficient $K_I$ were 0.28 mM and 18 mM, respectively. Since the substrate concentration used in this experiment was less than 1 mM, the product inhibition was considered to be negligible. Storage stability of the enzyme solution was investigated at 25°C. After checking the enzyme activity in free solution, the solution was recirculated by a bellow pump at 30 mL/min and its activities were determined by pipetting the aliquot. As can be seen in Figure 2, about 30% of the enzyme activity disappeared at the beginning probably owing to the favorable adsorption on the fiber and then

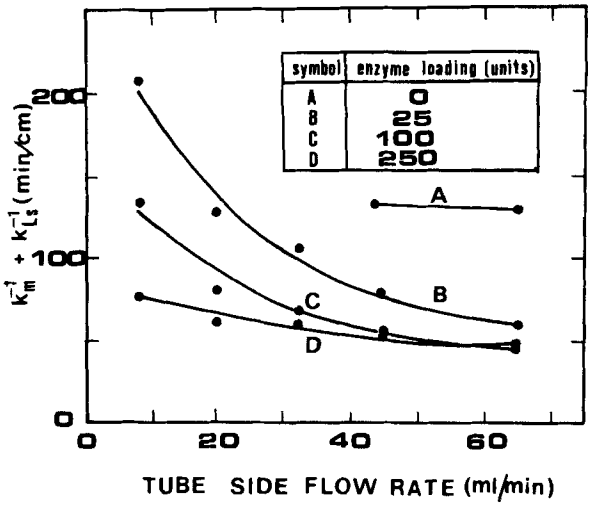


Figure 4. Decrease of resistance due to enzyme reaction in sponge region; feed concentration: 0.3 mM.

the enzyme activity decayed very slowly up to 120 hours. Therefore, it can be safely assumed the enzyme activity remains constant during one day period of the experiment. Figure 3 shows the permeability data for the H1P5 fibers obtained from dialysis experiments. We see that the permeability is dependent more on the shell side flow rate than on the tube side flow rate. The fiber has rather thick support membrane of 0.025 cm. The fluid contained in the sponge region is apt to become stagnant in spite of high flow rate in the shell.

Permeability enhancement due to the enzymic reaction is shown in Figure 4. According to Eqs. 2 and 3, $1/k_m + 1/k_{Ls}$ is represented by a function of the tube-side flow rate. As the enzyme loading is increased, the resistance comprised of the membrane ($1/k_m$) and the shell-side liquid film ($1/k_{Ls}$) diminishes. The effect of the flow rate on the sum of $1/k_m$ and $1/k_{Ls}$ is noticeable at a low enzyme loading. Waterland et al. (1975) discussed toroidal flow phenomena in the sponge region that stems from axial pressure drop along the fiber bundle. Fluids in the sponge annulus migrates axially and influences the membrane resistance at a low enzyme loading. In this case the reaction rate in the sponge region is slow, and the ultrafiltration effect is pronounced because of the high resistance of the sponge region. The flow dependency decreases when the reaction is nearly complete in the sponge region at a high enzyme loading. The hollow fiber membrane used in this study has an asymmetric structure comprised of the skin layer and the sponge region. To obtain the sponge region resistance, we pay attention to the resistance difference between $A$ and $D$ at 65 mL/min. The difference of 80 min/cm between $E = 0$ unit and $E = 250$ units is attributed to the sponge region resistance, since the skin layer and the shell-side liquid film have the same resistances for both cases. Using the data for the sponge thickness and the diffusivity of ONPG (Waterland et al., 1975), we can also estimate the sponge region resistance:

$$\text{resistance due to sponge} = \delta/D = \frac{0.025 \text{ cm}}{3.2 \times 10^{-4} \text{ cm}^2/\text{min}} = 77 \text{ min/cm}$$

This value is in good agreement with the experimentally observed value of 80 min/cm.

Figure 5 shows the conversion increase as the volume change of the shell side is enlarged. Here O.D. values are linearly correlated to the conversions as stated earlier. Increasing the amplitude of the inlet pulsatile flow leads to an increase of ultrafiltration; i.e., the ratio of convective to diffusive fluxes can be raised. According to the CSTR model by Kim and Chang (1983) the conversion en-

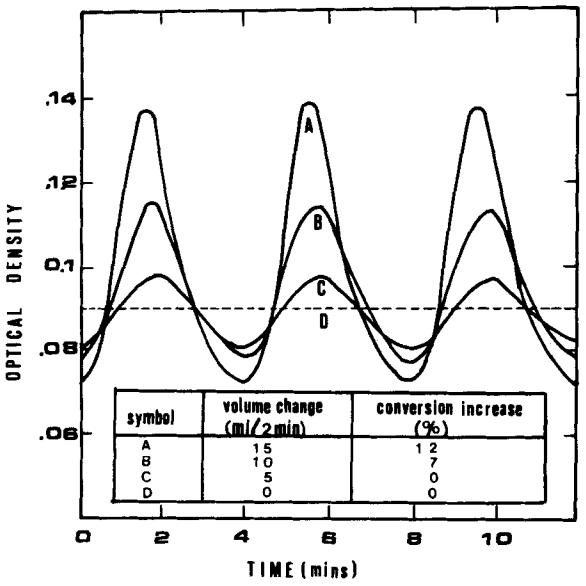


Figure 5. Effect of pulsatile flow amplitude on conversion increase: mean flow rate, 45 mL/min; enzyme loading, 50 units; feed concentration, 0.3 mM.

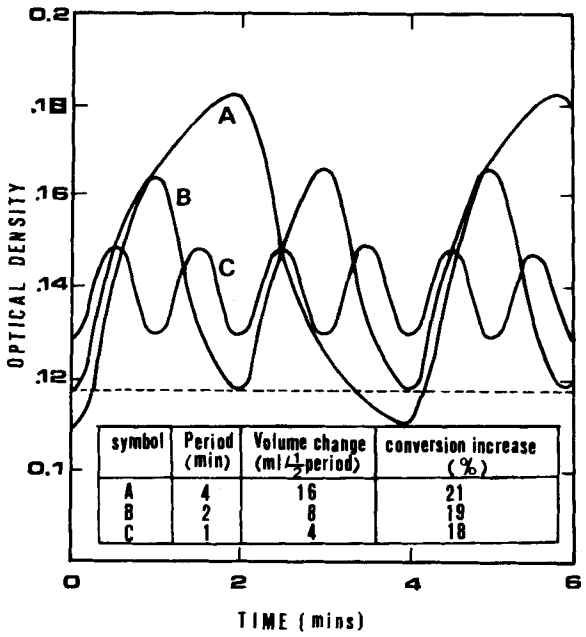


Figure 6. Effect of period on amplitude of concentration histories: mean flow rate, 23 mL/min; enzyme loading, 50 units; feed concentration, 0.3 mM.

hancement depends strongly on the parameter, $\beta$, defined as the ultrafiltration over the diffusion rates. Thus it is natural that the conversion increases as $\beta$ goes up.

The effect of the period with the same ultrafiltration rate is given in Figure 6. The amplitudes of concentration fluctuations become larger with the increase of the period. However, the conversion increase is so small that the effect seems to be insignificant, which was also predicted in the CSTR model (Kim and Chang, 1983).

Figure 7 shows concentration histories at different enzyme loading under the pulsatile flow conditions. The average O.D. values are higher than that of dotted lines obtained from the steady operations with the same average flow rate. The percent increase in conversion at $E = 250$ units is lower than that at $E = 25$ units due to the permeability increase, Figure 4, and the high steady conversion. Quantitative values are given in Table 1.

Figure 8 shows the conversion enhancements for the H1P10

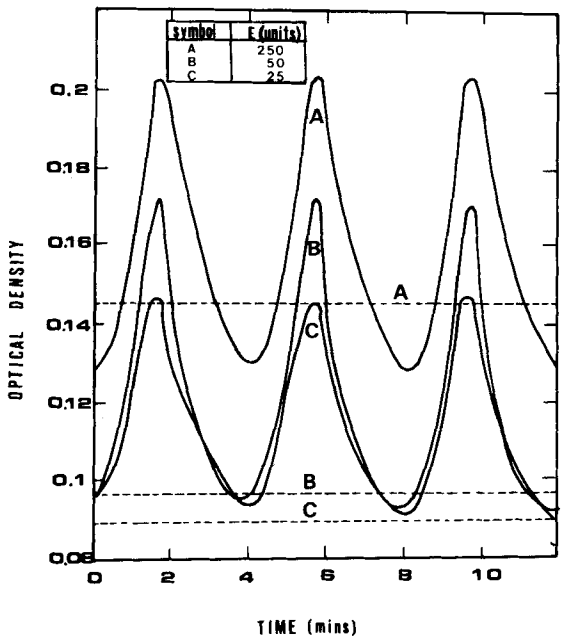


Figure 7. Steady and cyclic operations with variation of enzyme loading: mean flow rate, 44 mL/min; shell-side volume change during half period, 10 mL; feed concentration, 0.3 mM.

TABLE I. COMPARISON OF CONVERSION INCREASE AT TWO LEVELS OF ENZYME UNIT

| $E$ (Unit*) | $K_oA$ (cm$^3$/min) | $\beta$ | Conv. Increase (%) |
|---|---|---|---|
| 25 | 5.3 | 0.95 | 33 |
| 250 | 7.3 | 0.70 | 12 |

* 1 unit = 1 $\mu$mol of ONP produced per min at 25°C.

fiber. The increase in conversion is 20% at $S = 0.3$ mM and 15% at $S = 0.6$ and 0.9 mM. At a lower feed concentration, reactor operation is more diffusion-limited due to the closeness to the first-order kinetics; thus the conversion increase is more prominent.

## CONCLUDING REMARK

In the present investigations $\beta$ was kept at less than 1 because the maximum allowable operating pressure for H1P5 and H1P10 fibers were less than 1.7 atm. This limits ultrafiltration rate and consequently $\beta$. Although an improvement in conversion as high as 100% was expected according to the model of Kim and Chang (1983) on the CSTR case, this was not possible within the range of $\beta$ used in this study.

The comparison between the theory of Kim and Chang and the present experimental results was not made because the theory comes from a lumped CSTR model, and the experimental data were obtained in hollow fiber which is considered more or less to the plug-flow-type reactor and where the enzyme reaction occurs in the sponge annulus as well as in the shell side. This imples that the theoretical prediction of conversion increase in the hollow fiber enzyme reactor requires more elaborate analysis, i.e., a distributed model which considers the uneven distribution of enzyme in the sponge matrix and the outside of fibers. Another difficulty is that the kinetic properties of the adsorbed enzymes and the degree of adsorption are not known. This all makes the comparison difficult at this stage of the development for the variable-volume enzyme reactor. However, the theory based on CSTR model provides us with a conceptual model from which we can single out important parameters. The experiment has significance in that it proved that

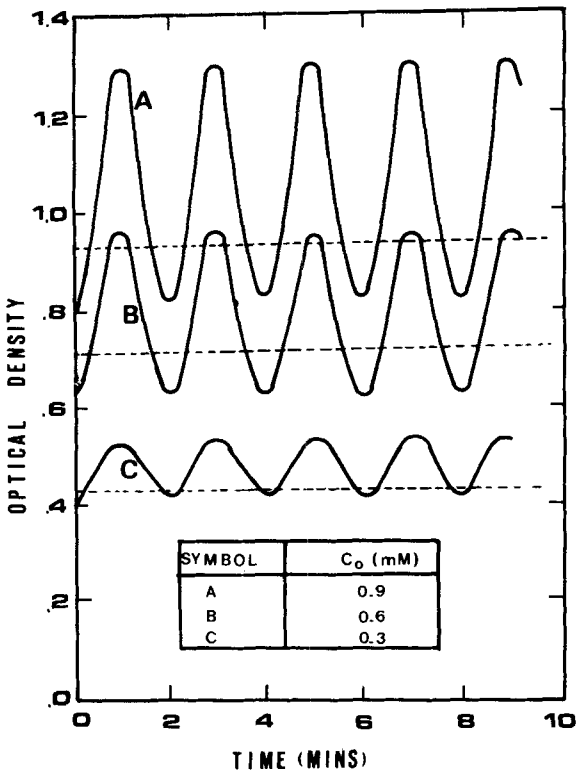


**Figure 8. Concentration histories with substrate concentration as a parameter: mean flow rate, 44 mL/min; enzyme loading, 250 units; shell-side volume change during half period, 20 mL.**

the conversion can be increased in membrane enzyme reactors by introducing ultrafiltration swing.

For the further study on the present convection-moderated membrane enzyme reactor, the following recommendations can be made:

(1) Model membrane enzyme reactor resembling a diffusion cell can be constructed to perform experiments in accordance with the CSTR model by Kim and Chang. However, the conversion obtained in this experiment may be very low because of the small membrane area in comparison with that of the hollow fiber reactor.

(2) To facilitate high ultrafiltration rate, porous membrane with large pores must be used. In this case soluble enzymes should be attached to microbeads large enough not to leak through the pores. Another possible application is to immobilize cells in the shell side and supply substrate by ultrafiltration swing. For example, if we use millipore HA type with pore size of 0.45 $\mu$m (Millipore, 1982), bacteria of 2 $\mu$m can be easily retained. The ultrafiltration rate is 39 cm/min at 25°C and 10 psi (69 kPa) and glucose permeability is 0.027 cm/min, from which we can obtain $\beta$ value as high as 1,450. In this case diffusion will be totally ineffective, and only ultrafiltration will contribute to the transport of the substrate. And presumably the cell leakages through the pores are less likely to occur than the asymmetric hollow fibers (Inloes, 1982).

## NOTATION

$A$ = total membrane area
$C_b$ = concentration in dense phase
$C_D$ = concentration in dilute phase
$C_o$ = inlet substrate concentration
$d$ = hollow fiber inner diameter
$D$ = molecular diffusivity of substrate
$E$ = enzyme unit
$k_L$ = liquid-film mass transfer coefficient
$k_m$ = membrane mass transfer coefficient
$K_m$ = Michaelis-Menten constant
$K_o$ = overall mass transfer coefficient
$L$ = effective length of hollow fiber
$Q$ = volumetric flow rate
$Re$ = Reynold number, $ud\rho/\mu$
$Sc$ = Schmidt number, $\mu/\rho D$
$S$ = substrate concentration
$t$ = time
$u$ = mean velocity parallel to axis of hollow fiber
$V$ = volume
$V_m$ = maximum reaction velocity
$x$ = coordinate along fiber axis

### Greek Letters

$\beta$ = ratio of ultrafiltration to diffusion rate
$\delta$ = thickness of sponge annulus
$\phi$ = parameter defined by Eq. 8

### Subscripts

$i$ = initial state
$s$ = shell side
$t$ = tube side

## LITERATURE CITED

Colton, C. K., K. A. Smith, E. W. Merrill, and P. C. Farrell, "Permeability Studies with Cellulosic Membranes," *J. Biomed. Mater. Res.*, **5**, 459(1971).

Inloes, D. S., "Immobilization of Bacterial and Yeast Cells in Hollow-Fiber Membrane Bioreactors," Ph.D. Thesis, Stanford Univ. (1982).

Kataoka, H., T. Saigusa, S. Mukataka, and J. Takahashi, "Effects of Axial Dispersion and Mass Transfer Resistances on Conversion in a Hollow Fiber Enzyme Reactor," *J. Ferment. Tech.*, **58**, 431(1980).

Kim, I. H., and H. N. Chang, "Variable Volume Enzyme Reactor with Ultrafiltration Swing—A Theoretical Study on CSTR Case," *AIChE J.* (1983).

Kim, I. H., "Effect of Ultrafiltration Swing on the Performance of a Hollow Fiber Enzyme Reactor," Ph.D. Thesis, KAIST, Seoul, Korea (1982).

Kohlwey, D. E., and M. Cheryan, "Performance of a $\beta$-D-galactosidase Hollow Fiber Reactor," *Enzyme Microb. Tech.*, **3**, 64(1981).

Ku, K., M. J. Kuo, J. Delente, B. S. Wildi, and J. Feder, "Development of Hollow-Fiber System for Large-Scale Culture of Mammalian Cells," *Biotech. Bioeng.*, **23**, 79(1981).

Lewis, W., and S. Middleman, "Conversion in a Hollow Fiber Membrane/Enzyme Reactor," *AIChE J.*, **20**, 1012(1974).

Millipore Laboratory Products Catalogue, Cat. No. MC 579, Millipore Corp., Bedford, Mass., pp. 35–37 (1982).

Rony, P. R., "Multiphase Catalysis II. Hollow Fiber Catalysis," *Biotech. Bioeng.*, **13**, 431(1971).

Rony, P. R., "Hollow Fiber Enzyme Reactors," *J. Amer. Chem. Soc.*, **94**, 23(1972).

Silman, R. W., L. T. Black, J. E. McGhee, and E. B. Bagley, "Hydrolysis of Raffinose in a Hollow-Fiber Reactor Using an Unrefined Mixture of $\alpha$-galactosidase and Invertase," *Biotech. Bioeng.*, **22**, 533(1980).

Waterland, L. R., A. S. Michaels, and C. R. Robertson, "A Theoretical Model for Enzymatic Catalysis Using Asymmetric Hollow Fiber Membranes," *AIChE J.*, **20**, 50(1974).

Waterland, L. R., C. R. Robertson, and A. S. Michaels, "Enzymatic Catalysis Using Asymmetric Hollow Fiber Membranes," *Chem. Eng. Com.*, **2**, 37(1975).

*Manuscript received March 29, 1982 and accepted December 17, 1982.*